Test bench for the characterization of two-phase passive immersion cooling of power electronic devices

Clément Hugon, Yvan Avenas, Samuel Siedel, Sébastien Flury

Test bench for the characterization of two-phase passive immersion cooling of power electronic devices

Clément HUGON[1,2], Yvan AVENAS[1], Samuel SIEDEL[2], Sébastien FLURY[1]
[1] Univ. Grenoble Alpes, CNRS, Grenoble INP, G2Elab, Grenoble, France
[2] Univ. Grenoble Alpes, CNRS, Grenoble INP, SIMAP, Grenoble, France

Abstract

Two-phase immersion cooling of power semiconductor devices receives a renewed interest thanks to the development of more environment-friendly phase-change and isolating fluids to extract increasing heat flux densities. In order to evaluate this cooling method, a thermo-sensitive electrical parameter is used to measure the temperature of power components during dissipation in condition close to actual ones. In this article, a test bench for the thermal characterization of pool boiling in HFE-7200 is presented as well as the measuring method, which gives an uncertainty on the temperature measurement lower than 0.44 °C. Thanks to this test bench, the thermal behaviour of immersed power devices can be characterized. Particularly, it allows measuring thermal resistance, maximal heat dissipation, and dynamic thermal response of devices.

Nomenclature

g	gravitational force equivalent, $m.s^{-2}$
I_C	collector current of IGBT, A
$I_{C\ SS}$	saturation collector current, A
L_v	latent heat of vaporisation, kJ/kg
P_{sat}	saturation pressure, Pa
q	surface heat flux density, W/m^2
R_{th}	thermal resistance, K/W
R_{shunt}	current measuring resistor, Ω
V_{CE}	collector-emitter voltage, V
V_{DC}	direct current voltage supply, V
V_{GE}	gate source voltage, V
V_E	voltage at the terminals of R_{shunt}, V
V_{ref}	reference voltage, V
T_j	junction temperature, °C
$T_{j,th}$	threshold junction temperature, °C
T_{sat}	saturation temperature, °C

Greek symbols

σ	surface tension, N/m
ρ	density, $kg.m^{-3}$

Indexes and exponent

l	liquid
v	vapour
c	critical

Acronyms

CHF	Critical Heat Flux
GDP	Global Depletion Potential
GWP	Global Warming Potential
IGBT	Insulated Gate Bipolar Transistor
MOSFET	Metal Oxide Semiconductor Field Effect Transistor
ODP	Ozone Depletion Potential
ONB	Onset Of Boiling
TSEP	Thermo-Sensitive Electrical Parameter
Cmd IGBT X	Command IGBT number X
Isolation X	Command MOSFET in series with IGBT number X

1 Introduction

With the increasing power of static converters, higher heat fluxes need to be evacuated. This is why new techniques are investigated to improve their thermal management. Currently air forced convection and cold plates are mainly used to extract heat from power semiconductor devices. Liquid-vapour phase change is more and more investigated in order to use its potential to extract heat from power electronics systems. This thermal exchange was already used to cool electric transformers in dielectric oil and to cool Insulated Gate Bipolar Transistors (IGBT) of inverters for high speed trains in Freon, which is now banned because of its high ozone depletion potential (ODP). FC72 was also mainly used [1]. Campbell et al. cooled an IGBT in a chopper configuration in R134a [2].

With the arrival of new fluids with zero ODP and low global warming potential (GWP), this cooling method experiences a new popularity. The latter are already used to cool datacenters [3] to dissipate low heat flux densities

(2W/cm^2) [4] but techniques are still investigated to improve heat transfers and reach higher heat flux densities which can be found in power electronics higher than 100W/cm^2.

In passive cooling, the best heat transfer coefficient are obtained in nucleate boiling regime. This boiling regime is bounded by the onset of boiling (ONB), when the first nucleation sites are activated, and by the critical heat flux (CHF), above which the heat transfer coefficient suddenly drops, leading to a dramatic increase of the component temperature and often a burn-out of the system.

The low thermal properties of these new fluids compared to older ones as R22 and R134a (see **Table 1**) lead to a lower CHF, an ONB reached for higher wall temperature and lower heat transfer. Therefore, many studies try to improve the surface properties in order to extend the nucleate boiling regime and to increase the heat transfer coefficients. For instance Sajjad et al. [5] study the thermal performance of different porous coating of Cu/Ni in saturated HFE-7200. To measure these performances, they use a copper block with heaters to provide the heat and a thermal isolation to avoid losses between the copper block and the liquid, several thermocouples in different places are used in order to calculate the heat flux. The tested surface is sintered to the copper block and a thermocouple in the porous surface is used to estimate the wall temperature. With this setup, they are able to calculate the surface heat flux density and the heat transfer coefficients on the tested surface. Jiang et al [6] use the same methodology to study sintered copper powder and mesh surfaces and calculate the pool boiling performances on these surfaces in saturated HFE-7100. The majority of the studies on the pool boiling performances of engineered surface are using the same method with heaters and thermocouples [7], [8]. These heaters, used to mimic power semiconductors, usually provide a homogeneous heat flux on the heat exchange surface. However, the heat dissipated by power semiconductors is non-homogeneous and leads to high temperature inhomogeneities on the heat exchange surface. Using a power semiconductor device itself as heat source could allow researchers to get closer to the real operating conditions of power semiconductors.

Furthermore, the strong temperature gradients and the strong integration of semiconductors components make the temperature measurement difficult with an external sensor. This temperature measurement can be done with thermosensitive electrical parameters (TSEP) of the semiconductor component. For example, Barnes and Tuma [9] investigate the pool boiling cooling of IGBT in HFE-7000. In order to measure the thermal performance of this cooling method, they use a TSEP, the saturation collector-emitter voltage ($V_{CE,sat}$). The temperature measured using this TSEP is called junction temperature (T_j) and represents an average temperature of the IGBT. The TSEP used by Barnes is measured at low collector current I_C (100 mA), which limits the applicability of the TSEP to measure Tj while operating at high heat fluxes that would require higher currents.

This article presents the test facility developed in order to characterize the thermal performance of several power semiconductor devices using saturated boiling cooling. The chosen TSEP, enabling the temperature measurement during heat dissipation, is detailed. The measuring circuit is presented as well as the method to calculate the junction temperature for any dissipated power. Applications linked to the advantages of this TSEP are given at the end.

2 Experimental setup and procedure

To study the cooling of semiconductor devices, the experimental apparatus for heat dissipation needs to be able to impose a constant temperature inside the sealed thermal enclosure. As there is an equilibrium between liquid and vapour phases, this temperature called saturation temperature (T_{sat}) corresponds to a pressure called saturation pressure (P_{sat}) which depends on the nature of the fluid.

2.1 Choice of the working fluid

The choice of the fluid is made among new dielectric fluids with no ODP and with a low GWP. The main issue is to find a fluid with the best thermal properties such as the specific enthalpy of vaporization L_v and the surface tension σ to maximize the theoretical critical heat flux. A low dielectric constant to avoid short circuit in the electric system and a high dielectric strength to avoid any breakdown between the different high potentials present in the system are also important properties.

Even if the theoretical CHF, given by Zuber's correlation ***(1)*** [10], increases with the saturation temperature, the range for the saturation temperature was chosen between 50°C and 100°C, to work with a pressure lower than 3 bar, which is less constraining for the vessel. This range corresponds as well to current cooling liquids for electric engines. q_c is the surface critical heat flux, ρ_v and ρ_l are respectively the mass density of the vapour and liquid phases and g the earth acceleration. According to these different parameters (**Table 1**), HFE-7200 was chosen among the different new fluids.

$$q_c = \frac{\pi}{24} L_v \rho_v \left(\frac{\sigma g (\rho_l - \rho_v)}{\rho_v^2} \right)^{1/4} \quad \textbf{(1)}$$

2.2 Sizing of the thermal enclosure

As the thermal enclosure aims to have an equilibrium between the vapour and liquid phases of the HFE-7200 for a range of saturation temperature between 50 °C and 100 °C, it needs to be sealed to primary vacuum and under pressure because the boiling temperature of HFE-7200 at 1 atm is 76°C. **Figure 1** shows a schematic view of the thermal enclosure. It includes a hermetic stainless steel cylinder of dimensions 500x160mm with a protuberance allowing the feedthrough of electric wires as well as the feedthrough of thermocouples. To maintain a constant saturation temperature, a thermostatic bath controls the saturation temperature with a Pt100 sensor and a condenser in the upper section supplied with water. The latter is sized in order to evacuate a heat flux of 1.2 kW for a complete power converter. To study the cooling of one component, which can

dissipate smaller heat flux, it is oversized and thus can maintain a constant saturation temperature. A 50 Ω heater resistor attached on the bottom perimeter of the cell can preheat the enclosure and maintain it at the chosen saturation temperature. An isolation wool around the walls avoids heat losses toward the ambient room, which helps to maintain a constant saturation temperature.

Properties	**HFE 7200 [11]**	**HFE 7100 [12]**	**HFE 7500 [13]**	**R134a [14]**	**R22 [14]**
P_{sat} (kPa)	16.4	26.9	2.29	665	1044
T_{sat} at ambient pressure	76	61	125	-26	-41
σ (N/m)	0.0136	0.0136	0.0162	0.0080	0.0081
L_v (kJ/kg)	125	112	89	178	183
ρ_l (kg/m^3)	1423	1400	1614	1207	1190
ρ_v (kg/m^3)	1.75	9.08	0.38	32.3	44.19
q_c (W/cm^2) (Zuber correlation)	8.4	16.2	2.9	41	27.6
Dielectric constant	7.5	7.4	5.8	9.24	6.11
Dielectric strength (kV/mm)	9.8	9.8	13.8	963	24
ODP	0	0	0	0	0.055
GWP	55	320	90	1430	1810

Table 1 Properties of HFE fluids, R134a and R22 at 25°C

A *Keysight DAQ973A* data recorder measures the temperature at different spots inside the cell with five T-type thermocouples to be aware of the saturation state between the vapour and liquid phases with an accuracy of 0.9 °C. A pressure sensor measures the pressure inside the cell to verify if the pressure corresponds to the saturation temperature of the two-phase mixture.
As there are high voltages in a power converter, the electrical feedthroughs support 1 kV between the different pins for the power supply and the measurement wires.

2.3 Experimental procedure

Before filling the enclosure with HFE-7200, a primary vacuum is carried out with a dedicated valve in order to remove most of air inside the cell and absorbed inside the walls. HFE-7200 is filled thanks to the pressure difference until the upper thermocouple of the liquid phase is completely immerged. Because there are still non-condensable gases inside, the mixture needs to be degassed to have a better control of the saturation temperature. It is heated up with the heating resistor and the condenser until the temperature of 78°C. At that temperature the pressure, if there is only HFE-7200 inside the cell, should be 1.095 bar. But, because of the non-condensable gases, the pressure is higher, so they can be removed thanks to an exhaust valve. Then the heat provided by the resistor is decreased to provide enough heat to compensate the losses across the isolated walls and the set point temperature of the external thermal bath is changed to the chosen saturation temperature. A primary study is needed to find the minimum power dissipated by the heating resistor, in order to maintain constant saturation temperature and to avoid heavy boiling inside the pool, which could impact the thermal behaviour on the tested component. Once the different temperatures in the cell are stable, the tests can be carried out. In steady state, the maximum gap between the different temperatures of the liquid and vapour phases is lower than four degrees.

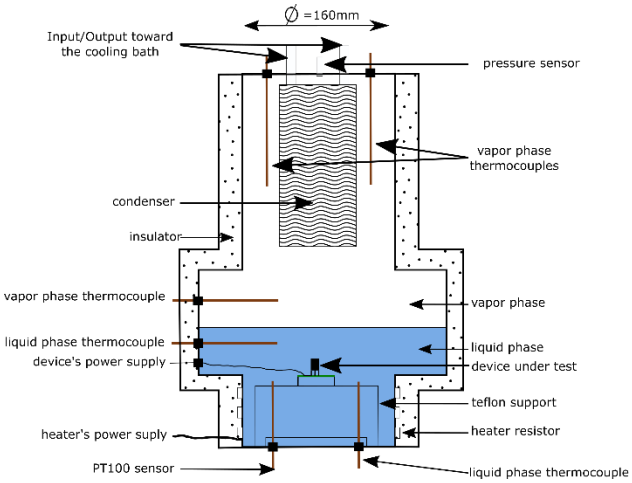

Figure 1 Schematic view of the experimental facility

3 Implementation of the temperature measurement

As mentioned before, a TSEP is used to measure the junction temperature of the component during heat dissipation. Each component having specific characteristics, the TSEP needs to be calibrated in order to evaluate its dependency on the temperature.

3.1 Choice of the thermo-sensitive parameter

Some TSEP can be measured while the component is dissipating a high heat flux whereas others can be measured only at low dissipated heat flux. **Figure 2** shows the schematic of an IGBT with its characteristic voltages and current. Either the saturation collector current $I_{C\,SS}$ or the collector-emitter voltage V_{CE} or the gate-emitter voltage V_{GE} can be used during high dissipation [15]. Among them, V_{GE} is the only TSEP, which is not linked to the power, thus the power can be maintained constant even if the temperature of the component is changing. This allows to study the thermal response to a power mission profile. In addition and contrary to V_{CE}, it can be used at low current (several Amps) for power dissipation in the range tens to hundreds of W, which facilitates its implementation in the test bench with less constraints on the feedthroughs and the electric connections. It also avoids boiling along the wires and on the printed circuit board (PCB) due to Joule heating.

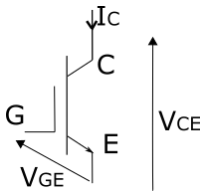

Figure 2 Schematic of an IGBT

In order to set the current I_C, a voltage V_{DC} is imposed across the tested IGBT and a resistor R_{shunt} in series (**Figure 3**). A secondary circuit controls the voltage V_E across the resistor R_{shunt} by comparing it with a reference voltage V_{ref} [16]. This external circuit applies a potential on the gate (G) of the IGBT to let it pass more or less current. The comparison is done with an OPA2277 operational amplifier for its low offset voltage drift (0.1 µV/°C), so that its output does not depend a lot on temperature. As its slew rate is low (0.8 V/µs), an asymmetrical power supply (+ 12 V / - 2 V) is used to shorten the delay between the command and the response. In order to have a current measurement, which does not change with room temperature, the resistor R_{shunt} is chosen with a maximal temperature coefficient of 15 ppm/K. This leads to an uncertainty on the current of +/-0.01 A. Moreover, to have a low heat dissipation in the resistor, a 0.1 Ω resistance value is chosen, leading to a dissipated heat of 0.4 W for a current I_C of 2 A.

Depending on the semiconductor device under test, oscillations on V_{GE} can appear because of its intrinsic capacitors, despite the low slew rate of the OPA, which makes this TSEP unusable for low power. Therefore, to avoid parasitic inductances, the OPA2277 is placed as close as possible to the component and in order to slow down even more the gate potential, a 1 kΩ resistor is added between the gate and the emitter. The power and the regulation circuits (called together measurement circuit in **Figure 3**) are thus located on the same PCB than the power device, and are therefore placed inside the pool boiling test bench. Four IGBTs can be calibrated and characterized separately, so there are four different regulation circuits on the PCB (not represented on **Figure *3***). In case of burn-out of a component, which leads to a short-circuit, a MOSFET (Metal Oxide Semiconductor Field Effect Transistor) is added in series in order to be able to isolate with the command "*Isolation X*" the damaged component from the other one. The latter can then be operated without removing manually the damaged component.

In order to choose either the calibration mode or the thermal characterization mode, and in order to select which IGBT is tested, another PCB with an *Arduino Nano* board is used and placed outside the pool boiling test bench. The two modes are chosen manually thanks to mechanical switches giving two digital inputs to the *Arduino* board, "*pulses*" and "*continuous*". "*pulses*" input corresponds to the TSEP calibration with the five 500 µs pulses and "*continuous*" input corresponds to the measurements in steady state inside the pool boiling test bench. The *Arduino* board drives an electronic switch (CD4016B) on the regulation circuit to turn on and off a given component with the commands "*Cmd IGBT X*". "*Cmd IGBT 1*" is set to one in order to switch on IGBT 1. The commands of the other IGBTs are set to zero to have a collector current of two Amps across IGBT 1. When the switch is in off-state, a negative voltage (-2 V) is imposed to the gate voltage thanks to a negative voltage source connected to the positive input of the OPA and to its asymmetrical power supply. When it is in on-state, the current in R_{shunt} is regulated and close to 2 A.

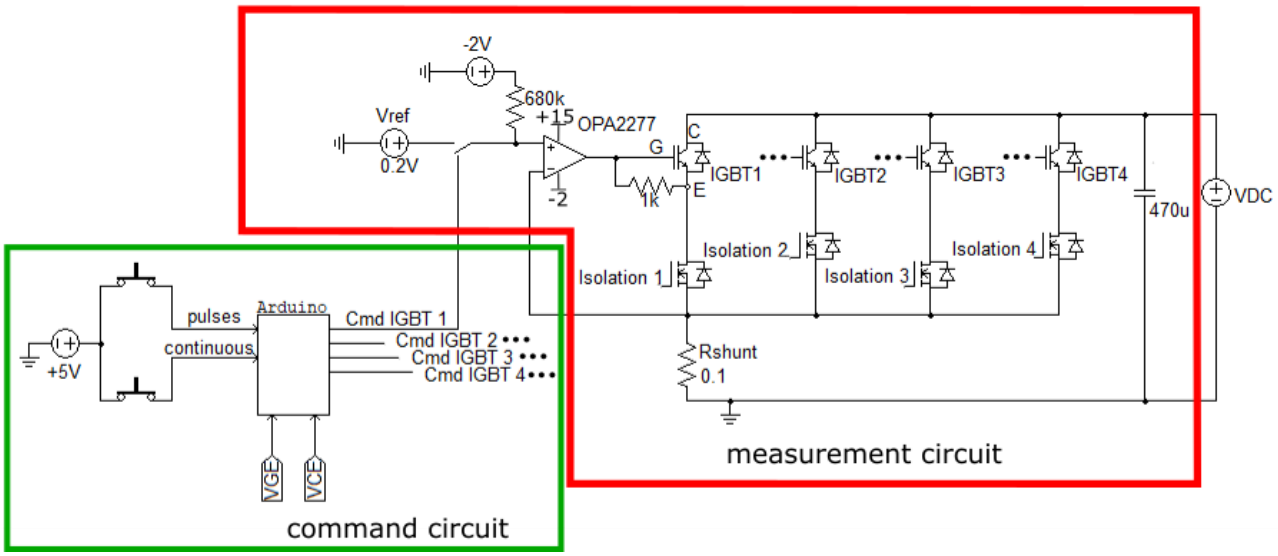

Figure 3 Electrical circuit for the TSEP measurement

On the control circuit, another circuit measures V_{GE} and V_{CE} and converts them to adapted analog inputs for the *Arduino Nano* board. Thanks to these measurements, a thermal protection, explained in the fourth part, is implemented.

To vary the dissipated power, the collector current I_C is set and the voltage V_{CE} is changed because the sensibility of V_{GE} on the current I_C is higher than its sensibility on the voltage V_{CE} (see **Figure 4**).

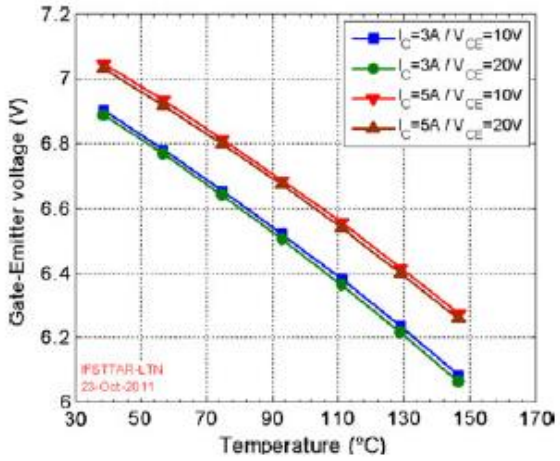

Figure 4 Characterisation of the parameter V_{GE} according to the junction temperature [7]

3.2 Calibration methodology

The junction temperature is set thanks to the combination of a hot plate, which heats up a copper block where the four components under test are screwed. A Pt100 sensor measures the temperature close to them in the block with a precision of 0.05 °C. This temperature in steady state is assumed as the junction temperature because of the low distance between the sensor and the components and because this calibration bench is thermally isolated. This TSEP is measured for a junction temperature from ambient to 150 °C. For each temperature set, once the temperature is stable, the control circuit of **Figure 3** imposes five 2 A pulses in the component. The duration of each pulse is 500 µs to limit self-heating. To start each pulse at the same junction temperature, a delay between them is set at 3 s. The voltage V_{DC} is fixed in a range between 2.5 V and 80 V. The voltage remains far lower than the breakdown voltage of the component – here FGH75T65SQD of $V_{CE\ max}$ = 650 V - and the dissipated power varies between 7 W and 160 W. V_{CE} and V_{GE} are measured during these pulses with a data recorder *HBM GEN 3i* with a sampling frequency of 1 MHz with an accuracy of 0.02%. Despite the short pulse duration, the component heats up. Thus an extrapolation needs to be done on the average of the five pulses to determine the initial voltage V_{GE} when the component is still at the temperature imposed by the hot plate [16].

Figure 5 presents the initial V_{GE} according to the junction temperature T_j for the different V_{DC} voltage tested. In order to estimate the accuracy of the temperature measurement the sensitivity of V_{GE} according to the temperature and V_{CE} are calculated. For the component FGH75T65SQD, the sensitivity of V_{GE} in relation to T_j is for example around - 7 mV/°C. The one in relation to V_{CE} is not constant and is higher for low V_{CE} (**Figure 6**).The maximal sensitivity of V_{GE} in relation to V_{CE} is -4 mV/V depending on the component.

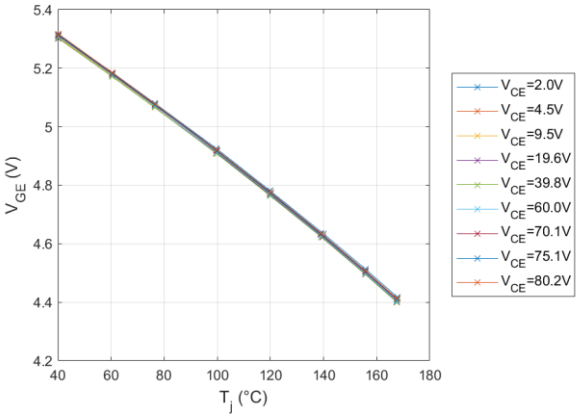

Figure 5 V_{GE} according to T_j for different V_{CE} for I_C = 2 A

During pool boiling characterization conditions, the current will be still set at the same value as for the calibration but as the heat flux will be increased gradually, the voltage V_{CE} will not be the same than during the calibration. Thus an interpolation is carried out to determine a function which links the temperature T_j for any couples (V_{GE}/V_{CE}). This relation will be valid for the same range for V_{GE} and V_{CE} as during the calibration.

3.3 Interpolation

The dependency of T_j on V_{GE} can be approached by a quadratic function [17]. **Figure 6** shows the low dependency of V_{GE} on V_{CE}. Zoomed, V_{GE} approaches a cubic polynomial function according to V_{CE}. Thus the interpolation function **(2)** is proposed. Then a least square method is used to obtain the different coefficients of this function. By this way, the junction temperature can be calculated for any V_{GE}/V_{CE} couple.

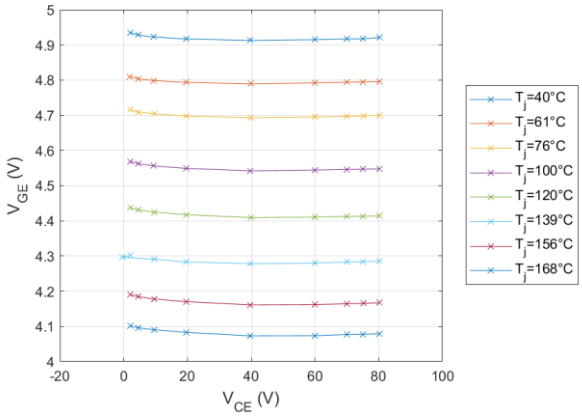

Figure 6 V_{GE} in function of V_{CE} for different values of T_j at I_C = 2 A

$$T_j = a_0 + a_1 V_{GE} + a_2 V_{CE} + a_3 V_{GE} V_{CE} + a_4 V_{CE}^2 + a_5 V_{GE}^2 + a_6 V_{CE}^2 V_{GE} + a_7 V_{CE} V_{GE}^2 + a_8 V_{CE}^3 \quad \textbf{(2)}$$

The interpolated temperature follows the measured temperature as **Figure 7** shows for three different voltages for reading reasons. The standard deviation between the interpolated and measured temperature T_j is around 0.2 °C. The accuracy of the data recorder being of 0.02 %, which leads to an uncertainty on V_{GE} and on V_{CE} of respectively around 1.2 mV and 16 mV. These uncertainties on the voltages causes a low uncertainty on T_j respectively 0.17 °C and 0.001 °C. It means that this method can provide an accurate estimation of the component temperature with an error on T_j of 0.44 °C. To keep the same conditions between the TSEP calibration and the temperature measurement, the same printed circuit boards with the same electronic components and the same recorder are used.

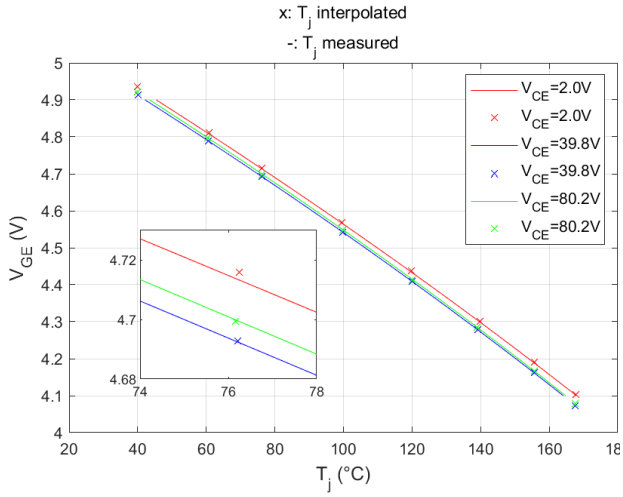

Figure 7 V_{GE} in function of interpolated and measured T_j for three different voltages for I_C = 2 A

the component can dissipate. In order to implement this thermal protection, on the control circuit (**Figure 3**), the Arduino calculates the junction temperature using **Equation (2)**. If this temperature exceeds $T_{j,th}$, the component is turned off. The program algorithm is shown in **Figure 8**.

$$R_{th} = \frac{T_j - T_{sat}}{V_{CE} I_C} \quad \textbf{(3)}$$

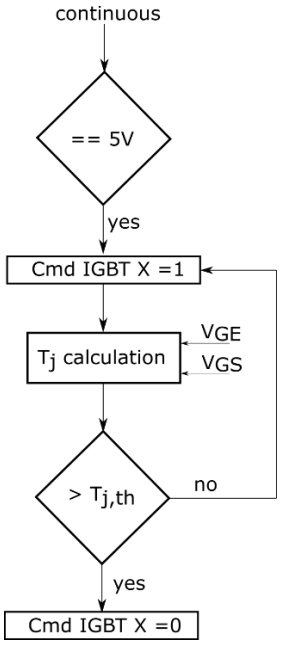

Figure 8 Program algorithm for the burn-out protection

4 Applications examples

4.1 Thermal resistance measurement

The TSEP chosen can be used to measure the thermal performance of direct immersion pool boiling cooling of IGBT. In particular, it can be used to help design optimized heat spreaders. The performance indicators selected are the global thermal resistance (R_{th}) and the maximal power that the component can dissipate. This thermal resistance characterizes the heat transfer between the component and the fluid at saturation. R_{th} is calculated using equation **(3)**, with T_{sat} the saturation temperature measured by the lower thermocouple in the liquid phase. When cooling power semiconductor devices, the operation conditions and especially the maximal thermal power dissipated are limited by the maximal temperature that the component can reach without damage. This maximal temperature can be reached either during nucleate boiling, if the heat flux density leads to a too high temperature superheat, or it can occur suddenly, if the CHF is reached as it would cause a dramatic surface temperature increase. Thus in order to prevent the component from burning-out, a threshold temperature $T_{j,th}$ is chosen beyond which the component is switched off. The dissipated power obtained at $T_{j,th}$ is the maximal power that

Figure 9 presents an example of thermal characterization of a power electronic device using the experimental facility and the measurement method detailed in the present manuscript. The thermal resistance of a given component on which a flat copper spreader in HFE-7200 at 59 °C. As expected, it can be observed that the thermal resistance decreases as the dissipated power increases in the fully developed boiling regime.

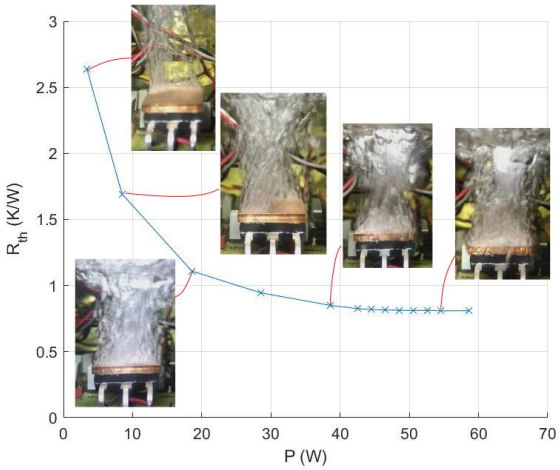

Figure 9 Thermal resistance during pool boiling

4.2 Dynamic response to a power step

In real operation condition, depending on the mission profile, the switched current across devices varies with time with possible quick changes. This may lead to fast change of their temperature. The TSEP chosen in the current method, contrary to the other possible candidates can be used to measure the dynamic thermal response of the junction temperature of a component to a power change, except if the power is close to zero Watt. **Figure 10** shows the thermal response to three different power steps from 0 W to respectively 8 W, 18 W and 37 W for a given component. In each case, an overshoot of temperature of T_j is observed, followed a temperature decrease and a stabilization which depends on the power level. This overshoot of temperature is due to the transition between natural convection cooling and boiling. Once the onset of boiling is reached, boiling spreads on the surface leading to a heat transfer enhancement. This temperature overshoot is no present in single-phase cooling, and can destroy the component for strong power steps, if the temperature reaches 175°C, the maximal temperature of the component. Using this method, contrary to the other TSEPs, the maximum power step supported by a component with its spreader without breaking can be measured.

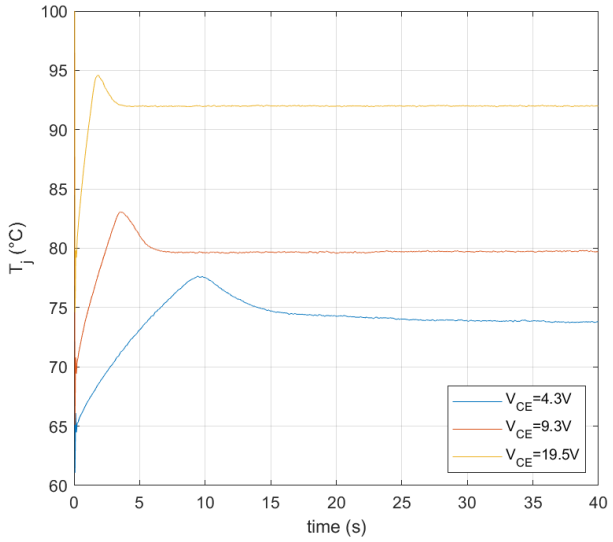

Figure 10 Dynamic response of T_j to a power step

5 Conclusion

In order to characterize the thermal behaviour of a semiconductor device during pool boiling cooling, a test facility has been developed in order to control the saturation temperature. The component itself is used to approach the real operating conditions. Therefore the TSEP V_{GE} has been used to estimate its junction temperature during its heat dissipation. This TSEP has been calibrate first for each device tested to obtain the junction temperature for any (V_{GE}/V_{CE}) couples for a current of 2 A. The voltage V_{CE} has not a big influence on the temperature measurement but the bigger uncertainty comes from the interpolation function with a standard deviation of 0.44 °C. This temperature measurement allows the obtaining of heat transfer performances during pool boiling such as the thermal resistance and a maximum dissipated heat flux in order to size heat spreaders. It allows as well to study the thermal response for different mission profiles. Thanks to this test bench, the thermal performances of different heat spreaders can be compare.

Acknowledgment

The authors would like to thank Institut Carnot Energies du Futur (MOSAIC project) for the funding of this research. The PhD grant of Clément Hugon is funded by the French Ministry of Education and Research.

6 Literature

[1] David Lossouarn, Alain Alexandre, and Michel Mermet-Guyennet, ‘Électronique de puissance & thermique dans le ferroviaire La voie diphasique’, Dec. 2005. [Online]. Available: https://www.sft.asso.fr/Local/sft/dir/user-3775/documents/actes/journeessft/JSFT_01-12-05/Ferroviaire-ALSTOM-LET.pdf

[2] Jeremy B. Campbell, Leon M. Tolbert, Curt W. Ayers, and Burak Ozpineci, ‘Two-Phase Cooling Method Using R134a Refrigerant to Cool Power Electronic Devices’, *Appl. Power Electron. Conf. Expo.*, 2005, doi: 10.1109/APEC.2005.1452904.

[3] 3M, ‘Two-Phase Immersion Cooling: A revolution in data center efficiency’. [Online]. Available: https://multimedia.3m.com/mws/media/1127920O/2-phase-immersion-coolinga-revolution-in-data-center-efficiency.pdf

[4] Mohamed S. El-Genk, ‘Immersion cooling nucleate boiling of high power computer chips’, *Energy Convers. Manag.*, vol. 53, pp. 205–218, Jan. 2012, doi: doi:10.1016/j.enconman.2011.08.008.

[5] U. Sajjad, A. Kumar, and C.-C. Wang, ‘Nucleate pool boiling of sintered coated porous surfaces with dielectric liquid, HFE-7200’, *J. Enhanc. Heat Transf.*, vol. 27, no. 8, pp. 767–784, 2020, doi: 10.1615/JEnhHeatTransf.2020035315.

[6] Y. Jiang, G. Zhou, J. Zhou, F. Zhou, and X. Huai, ‘Saturated pool boiling heat transfer of HFE-7100 on sintered copper powder and wire mesh microporous surfaces: A comparison study’, *Appl. Therm. Eng.*, vol. 216, p. 119067, Nov. 2022, doi: 10.1016/j.applthermaleng.2022.119067.

[7] Abhishek Kumar, Kuo-Shu Hung, and Chi-Chuan Wang, ‘Nucleate Pool Boiling Heat Transfer from High-Flux Tube with Dielectric Fluid HFE-7200’, *MDPI Energ.*, 2020.

[8] S. Sarangi, J. A. Weibel, and S. V. Garimella, ‘Effect of particle size on surface-coating enhancement of pool boiling heat transfer’, *Int. J. Heat Mass Transf.*, vol. 81, pp. 103–113, Feb. 2015, doi: 10.1016/j.ijheatmasstransfer.2014.09.052.

[9] C. M. Barnes and P. E. Tuma, ‘Immersion Cooling of Power Electronics in Segregated Hydrofluoroether Liquids’, *Am. Soc. Mech. Eng.*, Aug. 2008.

[10] T. L. Bergman and F. P. Incropera, Eds., *Fundamentals of heat and mass transfer*, 7th ed. Hoboken, NJ: Wiley, 2011.
[11] 3M, ‘datasheet HFE 7200’. [Online]. Available: https://multimedia.3m.com/mws/media/199819O/3m-novec-7200-engineered-fluid-en.pdf
[12] 3M, ‘datasheet HFE 7100’. [Online]. Available: https://multimedia.3m.com/mws/media/199818O/3m-novec-7100-engineered-fluid.pdf
[13] 3M, ‘datasheet HFE 7500’. [Online]. Available: https://multimedia.3m.com/mws/media/65496O/3m-novec-7500-engineered-fluid.pdf?&fn=prodinfo_nvc7500.pdf
[14] A. M. Gbur, ‘Determination of Dielectric Properties of Refrigerants’, *ASHRAE Trans.*.
[15] Y. Avenas, L. Dupont, and Z. Khatir, ‘Temperature Measurement of Power Semiconductor Devices by Thermo-Sensitive Electrical Parameters—A Review’, *IEEE Trans. Power Electron.*, vol. 27, no. 6, pp. 3081–3092, Jun. 2012, doi: 10.1109/TPEL.2011.2178433.
[16] D. P. U. Tran, S. Lefebvre, and Y. Avenas, ‘Discrete Power Semiconductor Losses Versus Junction Temperature Estimation Based on Thermal Impedance Curves’, *IEEE Trans. Compon. Packag. Manuf. Technol.*, vol. 10, no. 1, pp. 79–87, Jan. 2020, doi: 10.1109/TCPMT.2019.2939617.
[17] Y. Avenas and L. Dupont, ‘Evaluation of IGBT thermo-sensitive electrical parameters under different dissipation conditions – Comparison with infrared measurements’, *Microelectron. Reliab.*, vol. 52, no. 11, pp. 2617–2626, Nov. 2012, doi: 10.1016/j.microrel.2012.03.032.